Environment	Spread
Flat Rural	0.5 μs
Urban	5 μs
Hilly	20 μs
Mall	0.3 μs
Indoors	0.1 μs

Table 3.1: Typical delay spreads for various environments.

If $W > \frac{1}{\tau_{\text{ds}}}$, then the fading is said to be *frequency selective*, and $h(t;\tau)$ can no longer be replaced by a multiplication by the flat fading process $E(t)$ as in (3.12). The goal of this section is to study how the channel model should be modified to account for frequency selectivity.

3.5.1 CORRELATION MODELS FOR FREQUENCY SELECTIVE FADING

Recall that time-varying impulse response is given by

$$h(t;\tau) = \sum_n \beta_n e^{j\phi_n(t)}\ \delta(\tau - \tau_n) \tag{3.88}$$

where the phase process $\phi_n(t)$ evolves as:

$$\begin{aligned} \phi_n(t) &\approx \varphi_n + 2\pi\nu_n t \\ &= \varphi_n + 2\pi\nu_{\max} t\cos\theta_n \end{aligned} \tag{3.89}$$

with the phases $\{\varphi_n\}$ being i.i.d. Unif $[-\pi,\pi]$ (see Assumption 3.2 and (3.14)). We can rewrite (3.88) as

$$h(t;\tau) = \sum_n \beta_n e^{j\varphi_n}\ e^{j2\pi\nu_n t}\ \delta(\tau - \tau_n) \tag{3.90}$$

Before we develop a stochastic model for $h(t;\tau)$, we introduce two additional equivalent represensentations of the time-varying channel [Bel63].

Definition 3.11. *For a channel with impulse response $h(t;\tau)$, the time-varying transfer function is given by*

$$\begin{aligned} H(t;f) &= \int h(t;\tau)e^{-j2\pi f\tau}d\tau \\ &= \sum_n \beta_n e^{j\varphi_n}\ e^{j2\pi(\nu_n t - f\tau_n)} \end{aligned} \tag{3.91}$$

and the delay-Doppler spreading function is given by

$$\begin{aligned} C(\nu;\tau) &= \int h(t;\tau)e^{-j2\pi\nu t}dt\ . \\ &= \sum_n \beta_n e^{j\varphi_n}\ \delta(\nu - \nu_n)\ \delta(\tau - \tau_n) \end{aligned} \tag{3.92}$$

Statistical Characterization of $H(t;f)$

In characterizing the channel stochastically, it is easiest to deal with the time-varying transfer function $H(t;f)$ since it is written as a sum of complex exponentials (rather than impulses). Since H is a function of two variables, it must be modelled as a random *field*.

The contribution of the n-th path to $H(t;f)$ can be written as

$$\eta_n(t;f) = \beta_n e^{j\varphi_n}\ e^{j2\pi(\nu_n t - f\tau_n)} \tag{3.93}$$

Analogous to the result we derived earlier in the context of frequency flat fading (Result 3.2), $\eta_n(t;f)$ can easily be seen to be a zero-mean proper complex field.

The autocorrelation function (ACF) of the field $H(t;f)$ can be derived in a manner similar to the way in which we derived the ACF of the flat fading process in (3.20). In particular, we have

$$\mathsf{E}\left[H(t_1;f_1)H^\star(t_2;f_2)\right] \approx \sum_n \beta_n^2\ e^{j2\pi\nu_n(t_1-t_2)}\ e^{-j2\pi\tau_n(f_1-f_2)}\ . \tag{3.94}$$

Thus $H(t;f)$ is approximately stationary in both t and f, i.e., it is approximately a *homogeneous* random field. The homogeneous autocorrelation function can then be defined as

$$\begin{aligned} R_H(\xi;\zeta) &= \mathsf{E}\left[H(t+\xi;f+\zeta)H^\star(t;f)\right] \\ &\approx \sum_n \beta_n^2\ e^{j2\pi\nu_n\xi}\ e^{-j2\pi\tau_n\zeta}\ . \end{aligned} \tag{3.95}$$

Using the fact that $\nu_n = \nu_{\max}\cos\theta_n$, we can rewrite (3.95) as

$$R_H(\xi;\zeta) = \sum_n \beta_n^2\ e^{j2\pi\nu_{\max}\xi\cos\theta_n}\ e^{-j2\pi\tau_n\zeta} \tag{3.96}$$

We can express the autocorrelation function $R_H(\xi;\zeta)$ in terms a quantity, which is defined below, that is analogous to the Doppler power spectrum of (3.25):

Definition 3.12. *The delay-Doppler scattering function is given by*

$$\Psi(\nu;\tau) = \sum_n \beta_n^2\ \delta(\nu-\nu_n)\ \delta(\tau-\tau_n)\ . \tag{3.97}$$

The scattering function $\Psi(\nu;\tau)$ describes the distribution of power as a function of the Doppler frequency and delay. The discrete joint density of (3.97) can be approximated by continuous density, by considering the paths to be forming a *continuum*. As mentioned earlier, the continuous model is representative of diffuse scattering. The support of the scattering function is restricted to the rectangular region $[-\nu_{\max},\nu_{\max}]\times[0,\tau_{\rm ds}]$. Furthermore, the Doppler power spectrum $\Psi(\nu)$ is the marginal of $\Psi(\nu;\tau)$, i.e.,

$$\Psi(\nu) = \int_0^{\tau_{\rm ds}} \Psi(\nu;\tau)d\tau\ . \tag{3.98}$$

Based on (3.97), we can rewrite (3.96) as

$$R_H(\xi;\zeta) = \int_{-\nu_{\max}}^{\nu_{\max}}\int_0^{\tau_{\rm ds}} \Psi(\nu;\tau)\ e^{j2\pi\nu\xi}\ e^{-j2\pi\tau\zeta}\ d\tau d\nu \tag{3.99}$$

We may also express the autocorrelation function $R_H(\xi;\zeta)$ in terms of a power gain density. To this end, we generalize the angular gain density $\gamma(\theta)$ to a joint density that describes the allocation of power to both angle of arrival and delay.

Definition 3.13. *The joint angle-delay gain density $\gamma(\theta;\tau)$ is given by*

$$\gamma(\theta;\tau) = \sum_n \beta_n^2 \; \delta(\theta - \theta_n) \; \delta(\tau - \tau_n) \; . \tag{3.100}$$

Obviously, there is a one-one relationship between the scattering function, $\Psi(\nu;\tau)$, and the angle-delay gain density $\gamma(\theta,\tau)$. A straightforward change of variables argument yields

$$\gamma(\theta,\tau) = \nu_{\max} \sin\theta \; \Psi(\nu_{\max}\cos\theta,\tau) \; . \tag{3.101}$$

Based on (3.100), we can rewrite (3.96) as

$$R_H(\xi;\zeta) = \int_{-\pi}^{\pi} \int_0^{\tau_{\rm ds}} \gamma(\theta;\tau) \; e^{j2\pi\nu_{\max}\xi\cos\theta} \; e^{-j2\pi\tau\zeta} \; d\tau d\theta \tag{3.102}$$

WSSUS Model

The zero-mean proper complex field model for $H(t;f)$ implies that the time-varying transfer function, $h(t;\tau)$, and the delay-Doppler spreading function, $C(\nu;\tau)$, are both also zero-mean proper complex fields.

The autocorrelation function of $h(t;\tau)$ is easily shown to be

$$\mathsf{E}\left[h(t_1;\tau_1)h^\star(t_2;\tau_2)\right] = \left[\sum_n \beta_n^2 \; e^{j2\pi\nu_n(t_1-t_2)} \; \delta(\tau_1 - \tau_n)\right] \; \delta(\tau_1 - \tau_2) \tag{3.103}$$

Note that $h(t;\tau)$ is not a homogeneous random field since it is not stationary in the delay variable τ. However, it is indeed stationary in the time variable and *uncorrelated* in the delay variable. The continuous path generalization of this model for $h(t;\tau)$ is referred to as the Wide Sense Stationary Uncorrelated Scattering (WSSUS) model, and was first studied in great detail by Bello [Bel63]. For the continuous path generalization, we can rewrite autocorrelation function in terms of the delay-Doppler scattering function:

$$\mathsf{E}\left[h(t+\xi;\tau_1)h^\star(t;\tau_2)\right] = \left[\int_{-\nu_{\max}}^{\nu_{\max}} \int_0^{\tau_{\rm ds}} \Psi(\nu;\tau) \; e^{j2\pi\nu\xi} \; \delta(\tau_1 - \tau) \; d\tau d\theta\right] \delta(\tau_1 - \tau_2) \tag{3.104}$$

The autocorrelation function of the delay-Doppler spreading function, $C(\nu;\tau)$, is given by

$$\mathsf{E}\left[C(\nu_1;\tau_1)C^\star(\nu_2;\tau_2)\right] = \left[\sum_n \beta_n^2 \; \delta(\nu_1 - \nu_n) \; \delta(\tau_1 - \tau_n)\right] \; \delta(\tau_1 - \tau_2) \; \delta(\nu_1 - \nu_2) \; . \tag{3.105}$$

Thus, $C(\nu;\tau)$ is not stationary in ν or τ, but it is uncorrelated in both variables. Note that

$$\mathsf{E}\left[C(\nu_1;\tau_1)C^\star(\nu_2;\tau_2)\right] = \Psi(\nu_1;\tau_1) \; \delta(\tau_1 - \tau_2) \; \delta(\nu_1 - \nu_2) \; . \tag{3.106}$$

3.5.2 RAYLEIGH AND RICEAN FADING

As we did in the study of frequency flat fading, we first characterize the distribution of the time-varying transfer function for the situation where the scattering is purely diffuse, i.e., there is no specular component. The Central Limit Theorem (Result B.3) can be applied to obtain:

Result 3.10. *For purely diffuse scattering, $H(t;f)$ is well-modelled as a zero-mean, proper complex Gaussian random field.*

As a consequence, for fixed t, f, the magnitude $|H(t;f)|$ has a Rayleigh distribution and the phase $\angle H(t;f)$ is uniformly distributed on $[-\pi,\pi]$. The corresponding model for $h(t;\tau)$ is called the Gaussian WSSUS (or GWSSUS) model.

If there is a specular component (with possibly multiple paths) in addition to the diffuse paths, then we can write the time-varying transfer function as

$$H(t;f) = \sum_{n=1}^{N_s} \beta_n \, e^{j\varphi_n} \, e^{j2\pi(\nu_n t - \tau_n f)} + \tilde{\beta} \, \check{H}(t;f) \tag{3.107}$$

where $\check{H}(t;f)$ is a zero-mean, proper complex Gaussian, homogeneous field, and

$$\tilde{\beta}^2 = 1 - \sum_{n=N_s+1}^{N} \beta_n^2 \, . \tag{3.108}$$

Thus, $H(t;f)$ is a zero-mean, proper complex, homogeneous field, but is non-Gaussian. However, conditioned on $\varphi_1,\ldots,\varphi_{N_s}$, $H(t;f)$ is a proper complex, non-homogeneous field, with non-zero mean. Also, just as in the case of the flat fading process $E(t)$, for fixed t, f, the distribution of the envelope $|H(t;f)|$, conditioned on $\varphi_1,\ldots,\varphi_{N_s}$, is Ricean with Rice factor given in (3.71). If there is only one specular path, the unconditional distribution of $|H(t;f)|$ is also Ricean.

The time-varying impulse response and delay-Doppler spreading functions get modified in a similar fashion:

$$h(t;\tau) = \sum_{n=1}^{N_s} \beta_n \, e^{j\varphi_n} \, e^{j2\pi\nu_n t} \delta(\tau - \tau_n) + \tilde{\beta} \, \check{h}(t;\tau) \tag{3.109}$$

where $\check{h}(t;\tau)$ is a zero-mean, GWSSUS field.

$$C(\nu;\tau) = \sum_{n=1}^{N_s} \beta_n \, e^{j\varphi_n} \, \delta(\nu - \nu_n) \, \delta(\tau - \tau_n) + \tilde{\beta} \, \check{C}(\nu;\tau) \tag{3.110}$$

where $\check{C}(\nu;\tau)$ is a zero-mean Gaussian field that is uncorrelated in ν and τ.

Chapter 4

Sampled Delay-Doppler Channel Representations

4.1 INTRODUCTION

In this chapter we develop sampled representations for the time-varying channel $h(t, \tau)$. The motivation for such representations is that channel modeling independent of the signal space is irrelevant from a communication viewpoint — an effective channel *representation* commensurate with signal space characteristics is what is important. To this end, a fundamental understanding of the interaction between the signal space and the channel is critical. The sampled representations developed in this chapter precisely capture such interaction in temporal and spectral dimensions. In this context, the key signal space parameters are the signaling duration T and bandwidth W, whereas the key channel parameters are the delay spread, τ_{ds}, and the Doppler spread or Doppler bandwidth, $B_d = 2\nu_{\text{max}}$. We assume throughout this development that $T \gg \tau_{\text{ds}}$ and $W \gg B_d$.

The channel can be selective in time and/or frequency depending on the values for T, W, τ_{ds}, and B_d. Frequency selectivity is determined by the number of multipath components that can be resolved by the signal within the delay spread. The delay resolution is given by the signaling bandwidth: $\Delta\tau = 1/W$. The channel is said to be frequency non-selective if $\tau_{\text{ds}}/\Delta\tau = W \ll 1$ and frequency selective for $\tau_{\text{ds}}W \geq 1$. Time selectivity is determined by the number of Doppler shifts that can be resolved by the signal within the Doppler spread. The frequency resolution is given by $\Delta\nu = 1/T$. The channel is said to be time non-selective if $B_d/\Delta\nu = B_dT \ll 1$ and time selective for $B_dT \geq 1$. Strictly speaking, for $\tau_{\text{ds}}W \geq 0.2$ and $B_dT \geq 0.2$ there is sufficient selectivity in frequency and time, respectively, and must be taken into account [SA99].

4.2 DISCRETE-TONE APPROXIMATION FOR FREQUENCY-FLAT FADING

Recall from Section 3.4 that for frequency-flat fading, the channel input and output are related as

$$y(t) = E(t)x(t) \tag{4.1}$$

where

$$E(t) = \int_0^{\tau_{\text{ds}}} h(t,\tau) d\tau = \sum_n \beta_n \, e^{j\varphi_n} \, e^{j2\pi\nu_n t} \, . \tag{4.2}$$

It is clear from this equation that $E(t)$ is a linear combination of discrete tones at the Doppler frequencies of the paths. These tones may occur at any frequency in the range $[-\nu_{\text{max}}, \nu_{\text{max}}]$. This detailed description of $E(t)$ implicitly assumes an infinite resolution in the frequency domain, so that each path that contributes to $E(t)$ can be resolved in frequency. However, infinite resolution in the frequency can only be obtained by observing the process $E(t)$ over an infinite time horizon. This is not even approximately possible since our small scale variation model is valid only over time horizons of duration T_{small}, over which the path gains, delays, and angles of arrival remain roughly constant.

Consider modeling $E(t)$ over the interval $[0, T]$, where $T < T_{\text{small}}$. Then, using a Fourier series expansion, we can write

$$E(t) = \sum_{m=-\infty}^{\infty} c_m \, e^{\frac{j2\pi mt}{T}} \, , \; t \in [0,T] \tag{4.3}$$

where

$$\begin{aligned} c_m &= \frac{1}{T} \int_0^T E(t) \, e^{\frac{-j2\pi mt}{T}} \, dt \\ &= \sum_n \beta_n \, e^{j\varphi_n} \, \frac{1}{T} \int_0^T e^{j2\pi\nu_n t} \, e^{\frac{-j2\pi mt}{T}} \, dt \\ &= \sum_n \beta_n \, e^{j\varphi_n} \, e^{j\pi(\nu_n T - m)} \, \text{sinc}\left[T\left(\nu_n - m/T\right)\right] \end{aligned} \tag{4.4}$$

Thus $E(t)$ is expressed in terms of a series of equispaced Doppler frequencies. The resolution in frequency is of course $1/T$, and in particular, the paths that contribute to tap c_m are the ones that fall within the "sinc mask" at Doppler frequency m/T. While the representation of $E(t)$ in (4.3) is more structured than the path-wise description of given in (4.2), there are an infinite number of taps in sampled representation of (4.3). To further simplify the representation we exploit the bandlimitedness of $E(t)$.

As we saw in Section 3.4.5, the flat fading process $E(t)$ is strictly bandlimited to a maximum frequency of $\pm\nu_{\text{max}}$. We may define the two-sided bandwidth of $E(t)$ as:

Definition 4.1. *The Doppler bandwidth B_d is defined by*

$$B_d = 2\nu_{max} \, . \tag{4.5}$$

The product of the time horizon T and the Doppler bandwidth B_d determines the number of degrees of freedom (or the richness) in the flat-fading process $E(t)$. More specifically, let M be such that

$$2M + 1 = \lceil B_d T \rceil \, . \tag{4.6}$$

Then it is clear from (4.4) that the scattering contributes very little to taps c_m, with $m > M$ or $m < -M$. We can hence approximate the infinite sum of (4.3) by the finite sum

$$E(t) \approx \sum_{m=-M}^{M} c_m \, e^{\frac{j2\pi mt}{T}} \, , \; t \in [0,T] \tag{4.7}$$

The discrete tone approximation for $E(t)$ given in (4.7) is described pictorially in Figure 4.1.

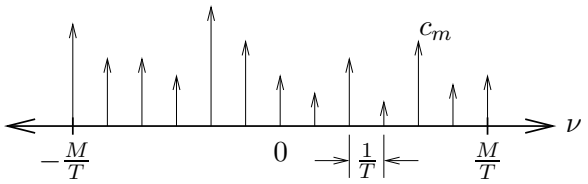

Figure 4.1: Discrete-tone approximation for frequency-flat fading

4.2.1 STATISTICAL MODEL FOR DOPPLER TAPS

The Doppler taps of (4.4) can be rewritten as

$$c_m = \sum_n \beta_n \, e^{j\varphi_n} \, e^{-j\pi m} \, \text{sinc}\left[T\left(\nu_n - m/T\right)\right] \;, \quad m = -M, \ldots, M \tag{4.8}$$

where we have absorbed the $e^{j\nu_n T}$ terms into the random phase terms $e^{j\varphi_n}$ without loss of generality.

Now, suppose the scattering is rich enough that the "sinc mask" corresponding to each tap captures a sufficiently large number of paths to apply the Central Limit Theorem. Further suppose that the scattering does not include a specular component. Then it follows that c_m has Rayleigh statistics, i.e., c_m is zero mean proper complex Gaussian, and that $|c_m|$ has a Rayleigh pdf. If there are one or more specular paths that contribute to c_m, then c_m has Ricean statistics. In calculating the Rice factor, the specular path gains contributing to c_m of course need to be scaled down by the "sinc mask" in (4.8).

Furthermore, using Assumption 3.2, the correlation between the taps is easily seen to be

$$\begin{aligned} \mathsf{E}[c_m c_k^\star] &= (-1)^{m-k} \sum_n \beta_n^2 \text{sinc}\left[T\left(\nu_n - m/T\right)\right] \text{sinc}\left[T\left(\nu_n - k/T\right)\right] d\theta \\ &= (-1)^{m-k} \int_{-\nu_{\max}}^{\nu_{\max}} \Psi(\nu) \, \text{sinc}\left[T\left(\nu - m/T\right)\right] \cdot \\ &\qquad\qquad \text{sinc}\left[T\left(\nu - k/T\right)\right] d\theta \end{aligned} \tag{4.9}$$

where $\Psi(\nu)$ is the Doppler power spectrum. Clearly the taps c_m are not independent in general.

4.2.2 CHANNEL ESTIMATION/PREDICTION AND TIME DIVERSITY

Note that with the discrete-tone approximation, we have captured the time variations in the random process $E(t)$ on the interval $[0, T]$ through (deterministic) complex exponentials, and the randomness is then captured by a finite set of random variables $c_m, m = -M, \ldots, M$. An immediate consequence of the finite Doppler sampled representation is that the fading process $E(t)$ can be perfectly estimated (or predicted) over the entire interval $[0, T]$ from a set of $2M + 1$ samples of $E(t)$ taken at distinct points in time. This has important implications for reliable digital communications on fading channels as we discuss below.

Consider sampling the fading process $E(t)$ in time with sampling interval T_s that is chosen such that

$$T_s \ll \frac{1}{B_d} \, . \tag{4.10}$$

In the context of digital communications on this flat fading channel, T_s could represent the symbol period, and condition (4.10) would then imply that the fading is *slow* relative to the symbol rate (see Definition 3.10). Under condition (4.10), the fading process $E(t)$ can be considered to be constant over intervals of duration T_s, so that we may represent $E(t)$ by the discrete-time process (sequence) $\{E_k\}$, with

$$E_k \stackrel{\Delta}{=} E(kT_s)\,, k = 0, 1, 2, \ldots\ . \tag{4.11}$$

In the following, we assume that $E(t)$ is a *Rayleigh* flat fading process, with the understanding that the extension to Ricean fading is straightforward. Suppose T_s is such that $T = KT_s$ for some integer K. Then, from (4.7) and (4.11), we obtain

$$E_k = \sum_{m=-M}^{M} c_m\, e^{\frac{j2\pi mkT_s}{T}} = \sum_{m=-M}^{M} c_m\, e^{\frac{j2\pi mk}{K}}\ . \tag{4.12}$$

From (4.12) it is clear that the rank of the covariance matrix of the vector $\boldsymbol{E} = [E_0\ E_1\ \cdots\ E_K]$ is at most equal to $2M + 1$. The ratio

$$\mu \stackrel{\Delta}{=} \frac{2M+1}{K} \tag{4.13}$$

is a measure of variation (equivalently, the predictability) of the channel. It is also a measure of the time diversity afforded by the channel that can be exploited to counter fading at the receiver through appropriate coding. From the slow fading condition (4.10) and (4.6), we get that

$$\mu = \frac{\lceil B_d T \rceil}{T/T_s} = \lceil B_d T_s \rceil \ll 1\,. \tag{4.14}$$

Thus slow fading channels can provide significant time diversity only over large block lengths. On the other hand, a small value of μ implies that long-range prediction of the channel is possible, and this could be exploited to advantage at the receiver.

4.3 TAPPED DELAY LINE MODEL FOR FREQUENCY-SELECTIVE FADING

In the previous section we exploited the finiteness of the time horizon to obtain a sampled Doppler representation of the channel. We now consider the dual problem of obtaining a sampled delay representation for frequency selective channels. To do so we exploit the bandlimitedness of the signal that is transmitted on the channel. For clarity of presentation, we do not assume sampling in the Doppler domain in this section. Joint delay-Doppler sampled representations will be the subject of the next section.

Referring back to Figure 3.14, since the channel input $x(t)$ has baseband bandwidth $W/2$ (and passband bandwidth W), by the Sampling Theorem (sinc interpolation formula) we can expand $x(t-\tau)$ as:

$$x(t-\tau) = \sum_{\ell=-\infty}^{\infty} x\left(t - \ell/W\right)\ \text{sinc}\left[W\left(\tau - \ell/W\right)\right] \tag{4.15}$$

Hence, starting with (3.5), we can express the channel output $y(t)$ in terms of $x(t)$ as:

$$\begin{aligned} y(t) &= \int_0^{\tau_{\text{ds}}} h(t;\tau)\, x(t-\tau) d\tau \\ &= \sum_{\ell=-\infty}^{\infty} x\left(t-\ell/W\right) \int_0^{\tau_{\text{ds}}} h(t;\tau)\, \text{sinc}\left[W\left(\tau-\ell/W\right)\right] d\tau \end{aligned} \tag{4.16}$$

We hence obtain the input-output relationship:

$$y(t) = \sum_{\ell=-\infty}^{\infty} x\left(t-\ell/W\right)\ E_\ell(t) \tag{4.17}$$

where

$$E_\ell(t) = \int_0^{\tau_{\text{ds}}} h(t;\tau)\, \text{sinc}\left[W\left(\tau-\ell/W\right)\right] d\tau\ . \tag{4.18}$$

To get a finite sampled representation, we exploit the fact that the range of the integrand τ in (4.18) is limited to $[0, \tau_{\text{ds}}]$ to obtain:

$$E_\ell(t) \approx 0 \text{ for } \ell < 0 \text{ and for } \ell/W > \tau_{\text{ds}} \tag{4.19}$$

Now, if we define

$$L = \lceil \tau_{\text{ds}} W \rceil\ , \tag{4.20}$$

then (4.17) simplifies to:

$$y(t) \approx \sum_{\ell=0}^{L} x\left(t-\ell/W\right) E_\ell(t) \tag{4.21}$$

Based on (4.21), we can see that we can replace the $h(t,\tau)$ of Figure 3.14 by the tapped delay line model shown in Figure 4.2, i.e.,

$$h(t;\tau) \approx \sum_{\ell=0}^{L} E_\ell(t)\ \delta\left(t-\ell/W\right) \tag{4.22}$$

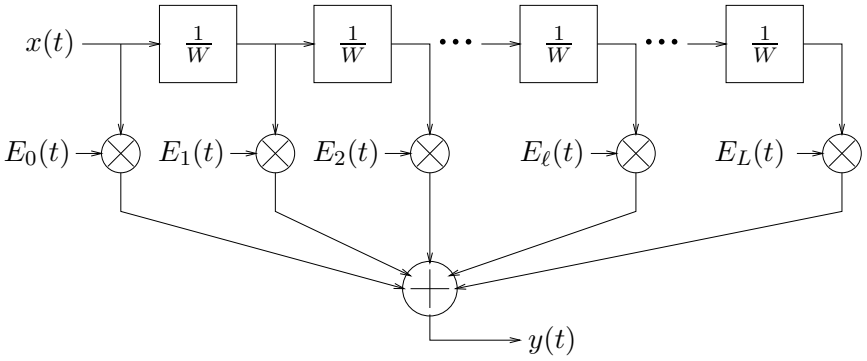

Figure 4.2: Tapped delay line model for frequency selective fading channel.

4.3.1 STATISTICAL MODEL FOR DELAY TAPS

Exploiting the fact that

$$h(t;\tau) = \sum_n \beta_n \, e^{j\varphi_n} \, e^{j2\pi\nu_n t} \, \delta(\tau - \tau_n) \, . \tag{4.23}$$

we can write $E_\ell(t)$ of (4.18) as:

$$E_\ell(t) = \sum_{n=1}^{N} \beta_n \, e^{j\varphi_n} \, e^{j2\pi\nu_n t} \, \mathrm{sinc}\left[W\left(\tau_n - \ell/W\right)\right] \, . \tag{4.24}$$

Note that $E_\ell(t)$ is similar in form to the flat fading process $E(t)$. The paths in the sum that contribute significantly to the process $E_\ell(t)$ are the ones that the "sinc mask" at delay ℓ/W picks out. Thus the frequency selective channel has been represented in terms of L flat fading processes.

Assume that the scattering is rich enough that there are a sufficiently large number of paths contributing to each delay tap to apply the Central Limit Theorem. Then, if $E_\ell(t)$ includes a specular component[1], it has Ricean statistics; otherwise, $E_\ell(t)$ has Rayleigh statistics.

The autocorrelation function (ACF) of $E_\ell(t)$ can be computed as follows:

$$\begin{aligned} R_{E_\ell}(\xi) &= \mathsf{E}\left[E_\ell(t+\xi)E_\ell^\star(t)\right] \\ &\approx \sum_n \beta_n^2 \, e^{j2\pi\nu_n\xi} \, \mathrm{sinc}^2\left[W\left(\tau_n - \ell/W\right)\right] \\ &= \int_0^{\tau_{\mathrm{ds}}} \int_{-\nu_{\max}}^{\nu_{\max}} \Psi(\nu,\tau) \, e^{j2\pi\nu\xi} \, \mathrm{sinc}^2\left[W\left(\tau - \ell/W\right)\right] \, d\nu \, d\tau \end{aligned} \tag{4.25}$$

where $\Psi(\nu,\tau)$ is the delay-Doppler scattering function of (3.97).

Remark 4.1. *If the fading is flat, i.e. $\tau_{ds} \ll \frac{1}{W}$, then $E_\ell(t) \approx 0$ for $\ell \neq 0$, and*

$$\begin{aligned} R_{E_0}(\xi) &\approx \sum_n \beta_n^2 \, e^{j2\pi\nu_n\xi} \, \mathrm{sinc}^2\left[W\tau_n\right] \\ &\approx \sum_n \beta_n^2 \, e^{j2\pi\nu_n\xi} \\ &\approx R_E(\xi) \end{aligned} \tag{4.26}$$

which is consistent with ACF derived in (3.21) *for flat fading.*

The form of $R_{E_\ell}(\xi)$ depends on angular location and spread of paths contributing to tap ℓ (see Figures 4.3 and 4.4). We can expect that as the number of taps increases (due to increasing bandwidth), the angular spread corresponding to each tap decreases, since each tap "sees" fewer paths. This would mean that the coherence time (see Definition 3.9) of each tap, and hence the coherence time of the frequency selective channel, is a strong function of the bandwidth W.

[1] Typically, only $E_0(t)$ will have such a component due to a LOS path.

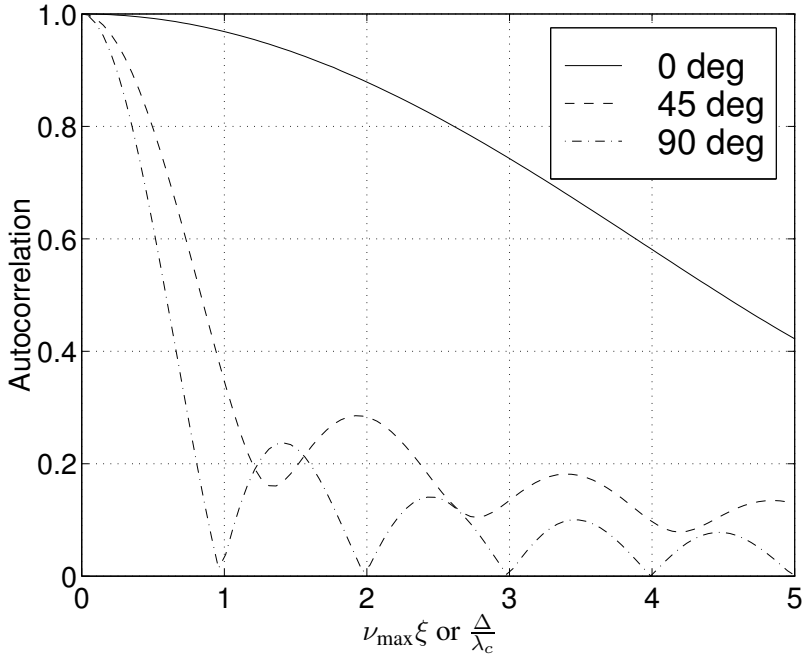

Figure 4.3: $0.5|R_{E_\ell}(\xi)|$ for various angular locations for spread of 60 deg.

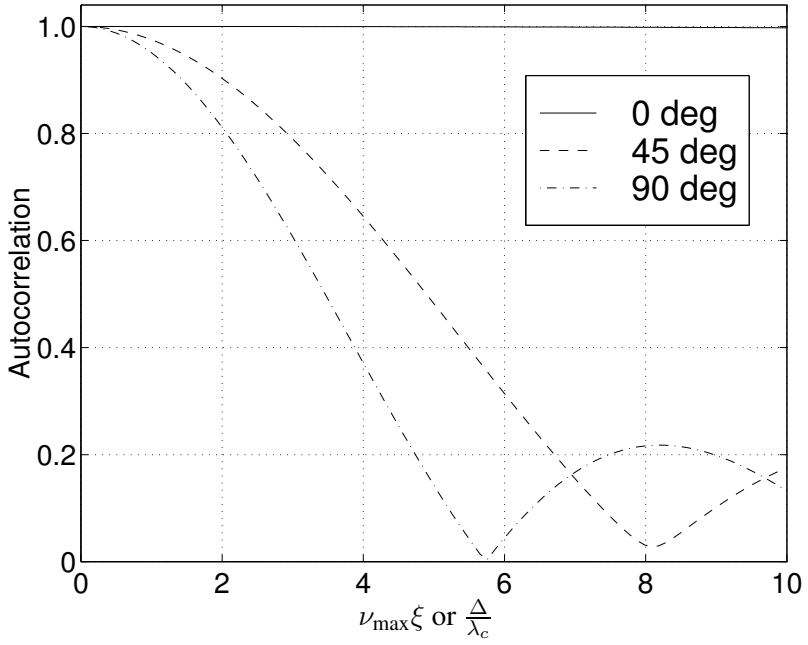

Figure 4.4: $0.5|R_{E_\ell}(\xi)|$ for various angular locations for spread of 10 deg.

It is also of interest to compute the cross-correlation function of $E_\ell(t)$ and $E_k(t)$, for $\ell \neq k$, since the frequency diversity afforded by the channel depends on cross-correlation between the taps.

$$\begin{aligned} R_{E_k E_\ell}(\xi) &= \mathsf{E}\left[E_k(t+\xi)E_\ell^\star(t)\right] \\ &\approx \sum_n \beta_n^2\, e^{j2\pi\nu_n\xi}\, \text{sinc}\left[W\left(\tau_n - \ell/W\right)\right]\, \text{sinc}\left[W\left(\tau_n - k/W\right)\right] \\ &= \int_0^{\tau_{\text{ds}}} \int_{-\nu_{\text{max}}}^{\nu_{\text{max}}} \Psi(\nu,\tau)\, e^{j2\pi\nu\xi}\, \text{sinc}\left[W\left(\tau - \ell/W\right)\right]\, \text{sinc}\left[W\left(\tau - k/W\right)\right]\, d\nu d\tau\ . \end{aligned} \tag{4.27}$$

From the above equation, one can see that the fading on neighboring taps can be correlated, except if the paths are clustered around the uniformly spaced tap centers.

If allow for flexibility in choosing the tap delays, instead of having them spaced uniformly in multiples of $1/W$, we get the following approximation:

$$h(t;\tau) \approx \sum_{\ell=0}^{L_c-1} E_\ell(t)\delta\left(\tau - \tau_\ell\right)\ , \tag{4.28}$$

where L_c is number of taps and τ_ℓ delay of tap ℓ. If the tap delays are chosen to match cluster centers in delay profile, then we get two beneficial outcomes. First, we may be able to approximate the channel with fewer taps, without wasting taps in portions of the delay profile that do not have significant received energy. Second, the taps will be more or less uncorrelated, i.e., $R_{E_k E_\ell} \approx 0$, for $\ell \neq k$.

4.3.2 JOINT DELAY-DOPPLER SAMPLED REPRESENTATION

In the previous section we developed a sampled delay representation for frequency-selective channels by exploiting the fact that we observe the channel over a finite bandwidth W. We now combine this sampled representation with the one developed in Section 4.2 for frequency-flat fading to obtain a joint delay-Doppler sampled representation of the channel.

Each of the taps $E_\ell(t)$ in the tapped delay line representation of (4.22) is bandlimited to a maximum frequency of $\pm\nu_{\text{max}}$, just as the flat fading process $E(t)$. As in Section 4.2, we assume that the channel is observed over a finite time horizon $[0,T]$, where $T < T_{\text{small}}$. Then each $E_\ell(t)$ has a sampled Doppler representation with $2M+1 = B_d T$ samples of the form:

$$E_\ell(t) \approx \sum_{m=-M}^{M} c_{m,\ell}\, e^{\frac{j2\pi mt}{T}}\ , \quad t \in [0,T]\ . \tag{4.29}$$

where

$$\begin{aligned} c_{m,\ell} &= \frac{1}{T}\int_0^T E_\ell(t)\, e^{\frac{-j2\pi mt}{T}}\, dt \\ &= \sum_n \beta_n\, e^{j\varphi_n}\, e^{-j\pi m}\, \text{sinc}\left[T\left(\nu_n - m/T\right)\right]\, \text{sinc}\left[W\left(\tau_n - \ell/W\right)\right]\ . \end{aligned} \tag{4.30}$$

Plugging approximation (4.29) into (4.22) yields the following approximate sampled representation for $h(t;\tau)$.

$$h(t;\tau) \approx \sum_{\ell=0}^{L} \sum_{m=-M}^{M} c_{m,\ell}\, e^{\frac{j2\pi mt}{T}}\, \delta\left(\tau - \ell/W\right)\ , \quad t \in [0,T]\ . \tag{4.31}$$

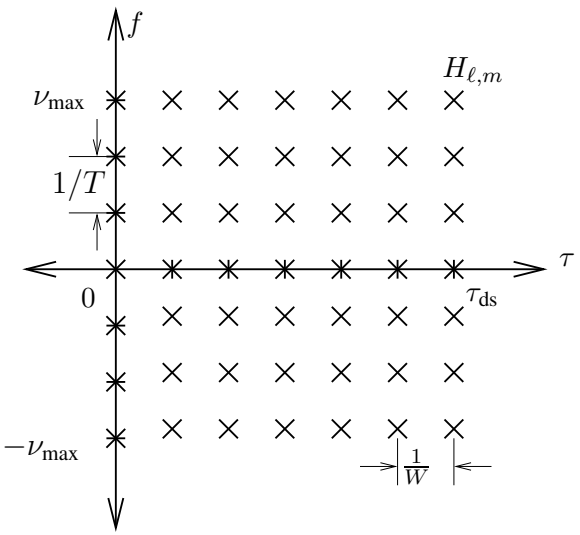

Figure 4.5: Canonical joint delay-Doppler sampled representation.

Note that the coefficients $c_{m,\ell}$ in the above sampled representation represent uniform sampling in delay and Doppler frequency. To further elucidate this point it is instructive to compare the sampled representation with the continuous delay-Doppler representation of $h(t;\tau)$ in terms of the spreading function $C(\nu,\tau)$ (see (3.92)).

$$h(t;\tau) = \int_0^{\tau_{\text{ds}}} \int_{-\nu_{\max}}^{\nu_{\max}} C(\nu;\tau)\, e^{j2\pi\nu t}\, \delta(t-\tau)\, d\nu\, d\tau \tag{4.32}$$

where

$$C(\nu,\tau) = \sum_n \beta_n e^{j\varphi_n}\, \delta(\nu-\nu_n)\, \delta(\tau-\tau_n)\,. \tag{4.33}$$

We now define $\widehat{C}(\nu,\tau)$ as a smoothed version of the spreading function imposed by the finite signaling duration and bandwidth, *viz.*

$$\widehat{C}(\nu,\tau) = \int_0^{\tau_{\text{ds}}} \int_{-\nu_{\max}}^{\nu_{\max}} C(\nu',\tau')\, e^{-j\pi T(\nu-\nu')}\, \text{sinc}(T(\nu-\nu'))\, \text{sinc}(W(\tau-\tau'))d\nu' d\tau'\,. \tag{4.34}$$

Then it is clear from the above equation and (4.30) that

$$c_{m,\ell} = \widehat{C}\,(m/T;\ell/W)\ . \tag{4.35}$$

Thus the representation of (4.31) is essentially a sampled version of (4.32) commensurate with the sampling resolution afforded by the signal space: $\Delta\tau = 1/W$, $\Delta\nu = 1/T$. Furthermore, the coefficients of the sampled representation are uniform samples of a smoothed version of the spreading function. The sampled delay-Doppler channel representation is illustrated in Figure 4.5).

4.3.3 STATISTICS OF THE SAMPLED REPRESENTATION

As we did previously in the case of sampled Doppler and sampled delay representations, we assume that the scattering is rich enough that the "sinc masks" corresponding to each coefficient in (4.30) capture a sufficiently

large number of paths[2] to apply the Central Limit Theorem. Under this assumption, if the paths contributing to $c_{m,\ell}$ do not include a specular component, then $c_{m,\ell}$ has Rayleigh first order statistics; otherwise, it has Ricean statistics.

The correlation between the coefficients is easily shown to be

$$\mathsf{E}[c_{m,\ell}c^{\star}_{m',\ell'}] = e^{-j\pi(m-m')} \int_0^{\tau_{\text{ds}}} \int_{-\nu_{\text{max}}}^{\nu_{\text{max}}} \Psi(\nu,\tau)\, \text{sinc}\left[T(\nu - m/T)\right]\, \text{sinc}\left[T(\nu - m'/T)\right] \cdot \\ \text{sinc}\left[W(\tau - \ell/W)\right]\, \text{sinc}\left[W(\tau - \ell'/W)\right]\, d\nu\, d\tau \tag{4.36}$$

From the above expression, we note that for sufficiently smooth $\Psi(\nu,\xi)$ (flat ideally), the correlation between different delay-Doppler coefficients is approximately zero as long as the indices are not too close to the end of their range. This follows from the orthogonality of the sinc basis functions.

The variation across blocks of duration T_{small} is much more complicated since it is governed by the large scale variations. A special case of such variations in discussed below.

Block (Independent) Fading Channel Model

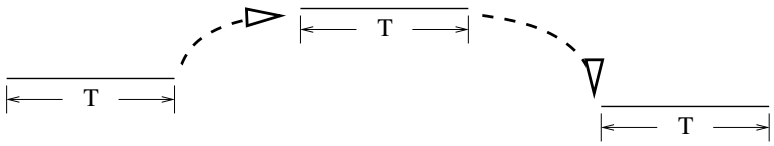

Figure 4.6: Block Fading Model

Consider the situation where the channel is observed over blocks of duration $T < T_{\text{small}}$, but channel realizations are independent from block to block. Such a scenario might arise in TDMA or frequency hopping systems, where consecutive blocks of the channel are well-separated in time or frequency. In this case the delay-Doppler coefficients remain constant over the each block, and change independently to new values from block to block. This model for fading is called the *block fading model*.

A special case of the block fading model is one where T is so small that $TB_d < 1$. This implies that one Doppler tap is sufficient, i.e., $M = 0$, and within each block

$$h(t;\tau) \approx \sum_{\ell=0}^{L-1} c_\ell\, \delta\left(\tau - \ell/W\right) \triangleq h(\tau)\,. \tag{4.37}$$

This means that the channel is LTI within each block. This special case of the block fading model has been used extensively in information-theoretic capacity calculations for fading channels.

The block (independent) fading model can be generalized to allow for both time-selectivity within the block ($TB_d > 1$) as well as correlation across blocks. Such a model would be useful in scenarios where independence cannot be justified using time or frequency hopping arguments. However, there could be spurious edge effects at the boundaries of blocks, and so one must be careful in developing such models.

[2]This assumption may not hold when T and (or) W are large even if the scattering is rich. We discuss this in greater detail in Section 4.4.